# Supporting Information

## Unveiling dissolution kinetics of CuO nanofertilizer using bio-based ionic liquids envisaging controlled use efficiency for sustainable agriculture

Mónia A. R. Martins[1-3], Leonard M. Kiirika[1], Nicolas Schaffer[4], Adam Sajnóg[5], João A. P. Coutinho[4], Gregory Franklin[1]*, Dibyendu Mondal[1,6]*

[1]Institute of Plant Genetics of the Polish Academy of Sciences, Strzeszyńska 34, 60-479 Poznan, Poland

[2]Centro de Investigação de Montanha (CIMO), Instituto Politécnico de Bragança, Campus de Santa Apolónia, 5300-253 Bragança, Portugal

[3]Laboratório para a Sustentabilidade e Tecnologia em Regiões de Montanha, Instituto Politécnico de Bragança, Campus de Santa Apolónia, 5300-253 Bragança, Portugal

[4]CICECO – Aveiro Institute of Materials, University of Aveiro, 3810-193 Aveiro, Portugal

[5]Department of Trace Analysis, Adam Mickiewicz University, Uniwersytetu Poznańskiego 8, 61-614, Poznań, Poland

[6]Centre for Nano and Material Sciences, Jain (Deemed-to-be University), Jain Global Campus, Kanakapura, Bangalore, Karnataka 562112, India.

*Corresponding author: Dibyendu Mondal, E-mail: dmon@igr.poznan.pl; m.dibyendu@jainuniversity.ac.in Gregory Franklin, E-mail: fgre@igr.poznan.pl

## Section I: Detailed experimental description

### *Synthesis of PGR-ILs*

PGR-ILs were synthesized by neutralizing cholinium carbonate with the appropriate acid, a well-established protocol that has been described in detail previously.[1,2] The choline cation was chosen because it is widely distributed in plant tissues and the anions are biomolecules that regulate plant growth. Briefly, the acids were suspended in ethanol and added dropwise to an excess of base under vigorous stirring room conditions, producing carbon dioxide and water. The mixture was allowed to stand for 24 hours with stirring and the lid open to remove the carbon dioxide formed. Unreacted starting materials were removed by liquid-liquid extraction with ethyl acetate. To reduce water content and volatile impurities, ILs were purified under vacuum (1 Pa) at room temperature with stirring for at least 48 h. The structure of the precursors and synthesized compounds was confirmed by $^{1}$H NMR (Nuclear Magnetic Resonance) spectra, and the synthetized ILs exhibited a 1:1 acid-base ratio along with a high degree of purity (Figure S1).

### *Materials characterization*

The PGR-ILs were characterized by $^{1}$H NMR in a Bruker Avance 300 at 75 MHz using deuterated water ($D_2O$) as solvent. Further manipulations on the purely synthesized compounds were performed in a glovebox with dry argon to avoid water absorption. CuO nanoparticles were characterized before and after dissolution experiments and contact with ILs using scanning Transmission Electron Microscopy (TEM) and powder X-ray diffraction (p-XRD). TEM analyses were performed using a Hitachi HD-2700 microscope at 200 kV and energy dispersive X-ray spectroscopy (EDS) using a Bruker Nano GmbH microscope. NPs were suspended in water and dispersed by sonication, and TEM grids were prepared by immersion. p-XRD measurements were performed at room conditions using an Empyrean X-ray diffractometer from PANalytical B.V. operating with a Cu anode (Kα1 = 1.5406 Å; Kα2 = 1.5444 Å) and equipped with a PIXcel$^{1D}$ detector. Diffraction data were collected in continuous mode in the 2θ range of 10-70° in steps of 0.04° and with a time per step of 295 s. Diffraction-free sample holders were used in the measurements. The pH was measured using a Mettler Toledo™ S470 pH benchtop meter. Cu ion concentration in aqueous solution containing PGR-ILs was quantified using a Picofox S2 (Bruker Nano, USA) total reflectance X-ray fluorescence spectrometer (TXRF) with a molybdenum X-ray source (X-ray tube voltage: 50 kV and current: 600 μA).

### *Experimental protocol to study the dissolution kinetics of Cu ions from CuO in PGR-ILs*

The release of copper ions from CuO was studied in ultrapure water and in the aqueous solutions containing [Cho][Asc], [Cho][IAA], [Cho][IBA], [Cho][$GA_3$], and [Cho][Sal] according to literature procedures.[3,4] Due to the expected low dissolution of copper ions, an approach adapted from previous work was implemented here,[5,6] in which dialysis tubing cellulose membranes act as 'filters' for particles of undissolved copper oxide. The dialysis membranes were previously humidified for at least 3 h with running water and subjected to pretreatment according to the manufacturer's instructions.[7] Then, one end of the dialysis tubing with a length of about 10 cm was closed with a double tight knot and the membranes were filled with the desired aqueous medium (water or water + PGR-IL). Copper oxide in excess was carefully added to the tubing attached to the plastic cover. The initial concentration of copper oxide and PGR-ILs used in each experiment are listed in Table S1. The system tubes + membranes containing 40 mL of ultrapure water and CuO + PGR-ILs were ultrasonicated for 2 min to desegregate the particles and then shaken at 200 rpm and 25°C in a Carousel 12 Plus reaction station. Aqueous samples of approximately 1 g were taken from the outside of the membrane after 1 h, 6 h, 12 h, 24 h, 72 h, and 168 h, diluted in 1 *wt*.% polyvinyl alcohol, and spiked with a known concentration of yttrium standard (1000 mg/L Certipur®standard, Sigma-Aldrich). 10 µL of each sample was then placed on a previously treated carrier (containing 10 µL of silicon in isopropanol solution) and dried on a hot plate at 353 K. Metal quantification was performed using a TXRF spectrophotometer with a molybdenum X-ray source (X-ray tube voltage: 50 kV and current: 600 µA). At least three independent measurements were made at each time point and in each solution, and the acquisition time was 500 seconds. The pH of the suspensions was measured before the experiment (in aqueous solutions of PGR-ILs) and after the end of the experiment (aqueous solutions of PGR-ILs and dissolved copper ions). Solutions containing [Cho][Asc] were evaluated by $^1$H NMR after 7 days, with the water peak suppressed by Bruker NMR software.

***Evaluation of the impact of Cu ion + PGR-ILs as foliar spray on tobacco (Nicotiana tabacum)***

*Preparation of nanoformulations*

To evaluate the effect on tobacco plant growth, the following treatments were prepared: (1) $H_2O$ (control), (2) $H_2O$ + CuO, (3) $H_2O$ + [Cho][Acs], (4) $H_2O$ + [Cho][IBA], (5) $H_2O$ + [Cho][$GA_3$], (6) $H_2O$ + [Cho][Sal], (7) $H_2O$ + [Cho][Asc] + CuO, (8) $H_2O$ + [Cho][IBA] + CuO, (9) $H_2O$ + [Cho][$GA_3$] + CuO, and (10) $H_2O$ + [Cho][Sal] + CuO. The suspensions containing copper oxide and/or ionic liquids were prepared by mixing the desired amounts (Table S2) with ultrapure water in Falcon tubes with a volume of 50 mL, allowed to stir for 6 days at room conditions, and filtered using 0.02 µm syringe filter units. For the subsequent greenhouse experiments, the filtration process is essential to separate the

dissolved Cu ions from the undissolved copper in the solution, since the goal is to determine the effect of the copper ions dissolved with the PGR-ILs. The formulations containing [Cho][IBA] were diluted 1000-fold after the filtration procedure. The potential degradation of PGR-ILs in the nanoformulations was evaluated after 3 months by $^{1}$H NMR following the procedure described in the previous section.

*Greenhouse experiments*

To test the efficiency of the nanoformulations based on Cu ions + PGR-ILs, tobacco seeds (*N. tabacum* L. cv Petit Havana) were germinated under *in vitro* conditions as described in Štefanić et al.[8] with minor modifications. Briefly, seeds were surface sterilized with 70% (v/v) ethanol for 60 seconds, washed 3x with sterile deionized $H_2O$, and soaked in 50% (v/v) sodium hypochlorite with an active chlorine concentration of 1.5% for 6 minutes before being rinsed 3x in sterile deionized $H_2O$. Seeds were then germinated on half-strength Murashige and Skoog (MS)[9] culture medium supplemented with 15 g $L^{-1}$ sucrose. Tobacco seedlings were then planted in pots (3 seedlings per pot) with sterile peat substrate and maintained under greenhouse conditions (16/8 light/dark cycle, light intensity 90 µmol $m^{-2}$ $s^{-1}$, 70% RH, and temperature 24°C). The experiment was conducted in a randomized complete block design (RCBD) with three replicates. Seedlings were allowed to grow for up to 19 days and sprayed with different Cu ions + PGR-ILs -based nanoformulations four times at one-week intervals until the end of the experiment. Each pot received approximately 1 g of the nanoformulations per treatment, as calculated from the mass difference before and after spraying. The control was treated with ultrapure water without any nanoformulations. Prior to application, plants were checked for uniformity, well-developed shoots, and differentiated leaves. Pots were watered to field capacity (3.5 ml $g^{-1}$ substrate) throughout the experiment.

*Study of plant growth*

The effect of nanoformulations on plants was evaluated 1 week after each foliar application by observing plant phenotype, which included plant height above ground, number of true leaves, and leaf area. Data were collected at time points t-0, t-7, t-14, t-21, t-28, and t-35 from the first day of foliar application. The designations t-0, t-7,..., t-35 are used to indicate the time point, where t-0 corresponds to the day of the first spray, and t-35 the last day of treatment. At the end of the experiment (8 weeks after sowing), the roots and shoots were harvested. The roots and shoots were rinsed with tap water followed by distilled water. After removing the excess water with filter paper, the fresh weight was measured. Plant samples were dried at 65 °C in a forced-air oven for 48 h to determine dry biomass yield. Phenotypic data were collected in triplicate for each treatment. Images

of plant shoots and roots were also taken to qualitatively evaluate the effects of the different treatments.

*Chlorophyll index and gas exchange parameters*

Chlorophyll index in leaves was measured nondestructively using a portable SPAD-502Plus Chlorophyll Meter (Konica Minolta GmbH). Leaf photosynthetic efficiency was measured on individual plants per treatment and sampling point, for all treatments at three time points (t-7, t-14, t-21), and at each foliar spray. Photosynthetic parameters were measured in triplicate for each plant considering actively growing leaves, with 9 measurements per treatment. Gas exchange parameters such as net photosynthetic rate $P_N$ (µmol $CO_2$ $m^{-2}$ $s^{-1}$), transpiration $T_r$ (mmol $H_2O$ $m^{-2}$ $s^{-1}$), conductance Cond (mol $H_2O$ $m^{-2}$ $s^{-1}$), and intercellular $CO_2$ concentration Ci (µmol $CO_2$ $mol^{-1}$) were measured using a LI-6400XT Portable Photosynthesis System (LI-COR Biosciences) on a leaf in the same position on each plant (one plant per treatment). Measurements were made under artificial light conditions in the chamber at an intensity of 750 µmol $m^{-2}$ $s^{-1}$, 400 µmol $mol^{-1}$ $CO_2$ with a flux of 200 µmol $s^{-1}$, and 50-65% RH. The instrument was recalibrated after each measurement of 15 samples to obtain stable readings.

*Copper mapping*

After harvesting, a fresh leaf was selected at the same position on each plant (1 per treatment, second true leaf from the base/bottom of the plant), and preserved according to the herbarium method. After complete drying, a rectangular area of about 0.5-1 cm x 1 cm of each leaf was fixed on the double-sided tape before ablation. An inductively coupled single quadrupole plasma mass spectrometer (ICP-MS) instrument 7700x (Agilent, Santa Clara, CA, USA) and a laser ablation (LA) system LSX-500 (CETAC Technologies, Omaha, NE, USA) were used for copper mapping. The LA-ICP-MS was optimized prior to analysis by ablation of certified glass NIST 610 reference material to achieve the required sensitivity and oxide and double charged ion content < 0.5%. Laser ablation parameters were selected using a single digit method while a leaf sample was ablated. The resulting instrumental parameters of LA-ICP-MS are as follows: laser energy 50%, laser scanning speed 400 µm $s^{-1}$, laser spot size 200 µm, distance between lines 400 µm, laser shot frequency 4 Hz, sample gas (argon) 1 mL $min^{-1}$, plasma power 1550 W, and acquisition time per mass per reading 50 ms. The isotopes observed were $^{13}C$ and $^{63}Cu$. The background signal measured before the start of ablation was subtracted. The $^{63}Cu$ signal was normalized to the $^{13}C$ signal to minimize signal fluctuations caused by variable sample thickness and instrumental drift. The double-sided tape was checked for copper content, that was found to be negligible (normalized signal Cu/C < 0.1). Data were processed using MS Excel 2021, and maps were generated using ImaJar software developed in-house (Robin Schmid, University of Münster).

*Elemental analysis and copper content of leaves*

Dried root and shoot tissues were ground into powder using a homogenizer (Taurus, 25 790 Barcelona, Spain) and passed through a 1 mm sieve to obtain a fine powder. Elemental content, including C, H, N, and S, was measured in the ground powder using a CHNS analyzer (Leco Truspec-Micro CHNS 630-200-200). Root and shoot tissue carbon content was used in conjunction with dry biomass yield to calculate the extent of $CO_2$ sequestration. Similarly, N content was used to calculate crude protein content, by %N x 6.25.[10] In addition, Cu content of shoots and roots was quantified using TXRF as described above.

*Statistical analysis*

The data obtained from pH, phenotypic, and physiological studies was statistically analyzed using paired sample T-test in OriginPro 2023 software (OriginLab Corporation, United States). The paired sample T-test revealed significant differences (with the level of significance set at $p < 0.05$) between treated plants and the control for various parameters, including leaf area, chlorophyll index, gas exchange parameters, dry biomass content, $CO_2$ sequestration, and crude protein content.

## Section II: Precursors and synthetized ionic liquids characterization

### $^{1}$H NMR

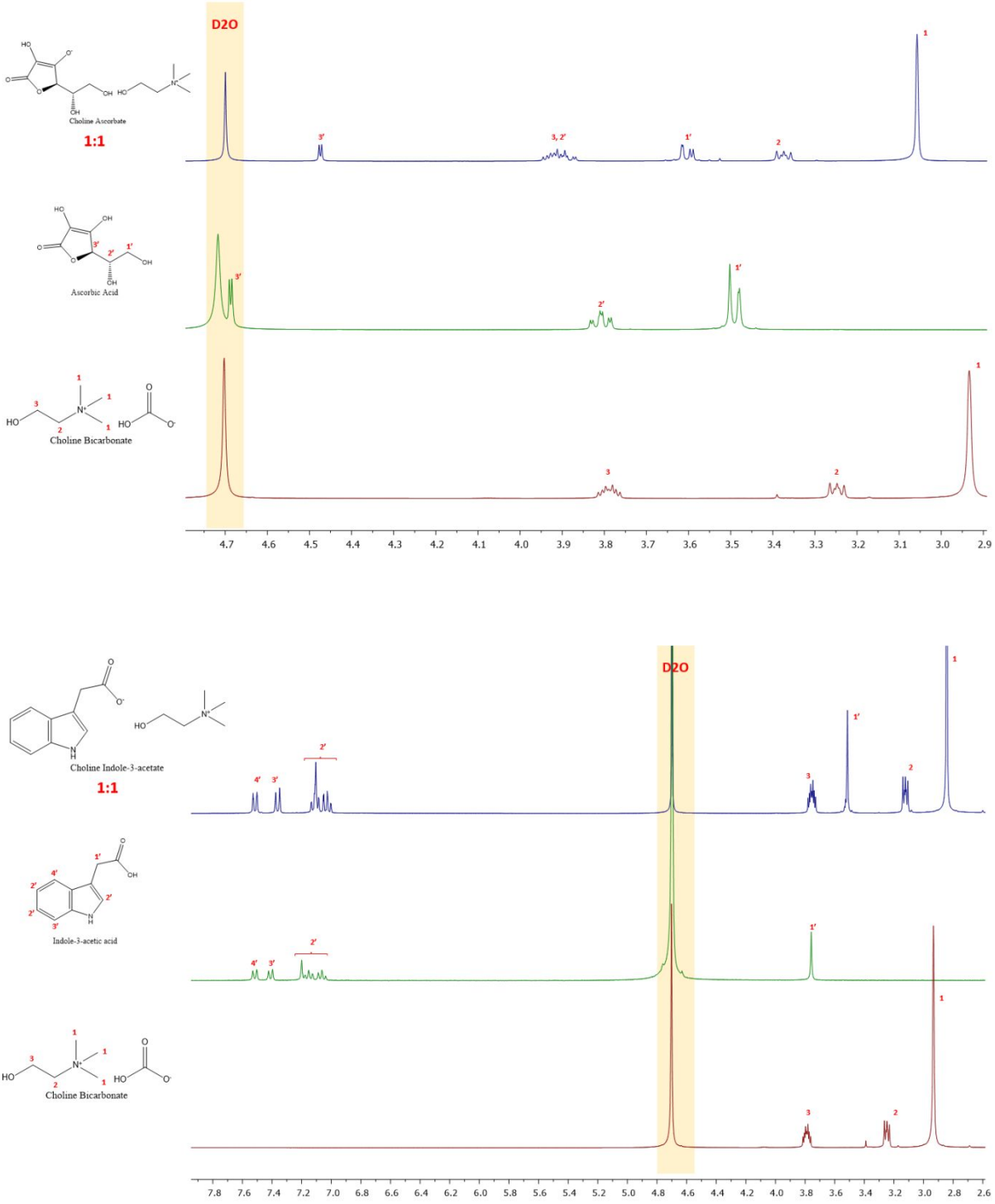

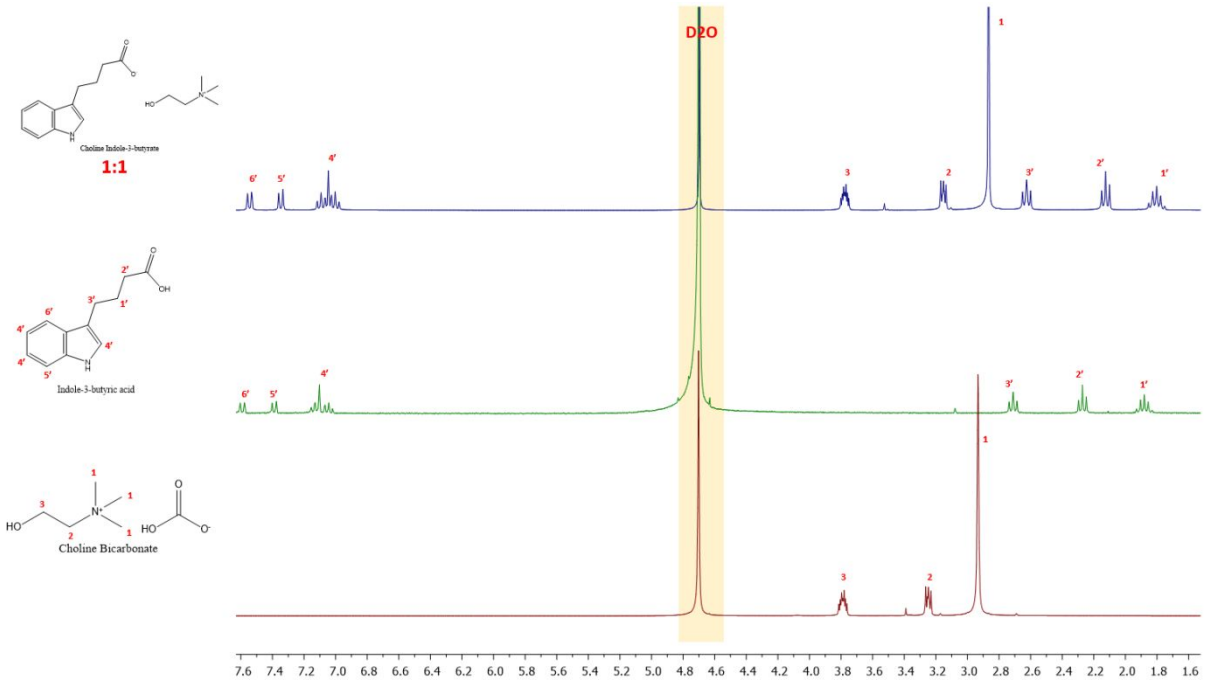
Choline Indole-3-butyrate
1:1
Indole-3-butyric acid
Choline Bicarbonate
D2O
7.6 7.4 7.2 7.0 6.8 6.6 6.4 6.2 6.0 5.8 5.6 5.4 5.2 5.0 4.8 4.6 4.4 4.2 4.0 3.8 3.6 3.4 3.2 3.0 2.8 2.6 2.4 2.2 2.0 1.8 1.6

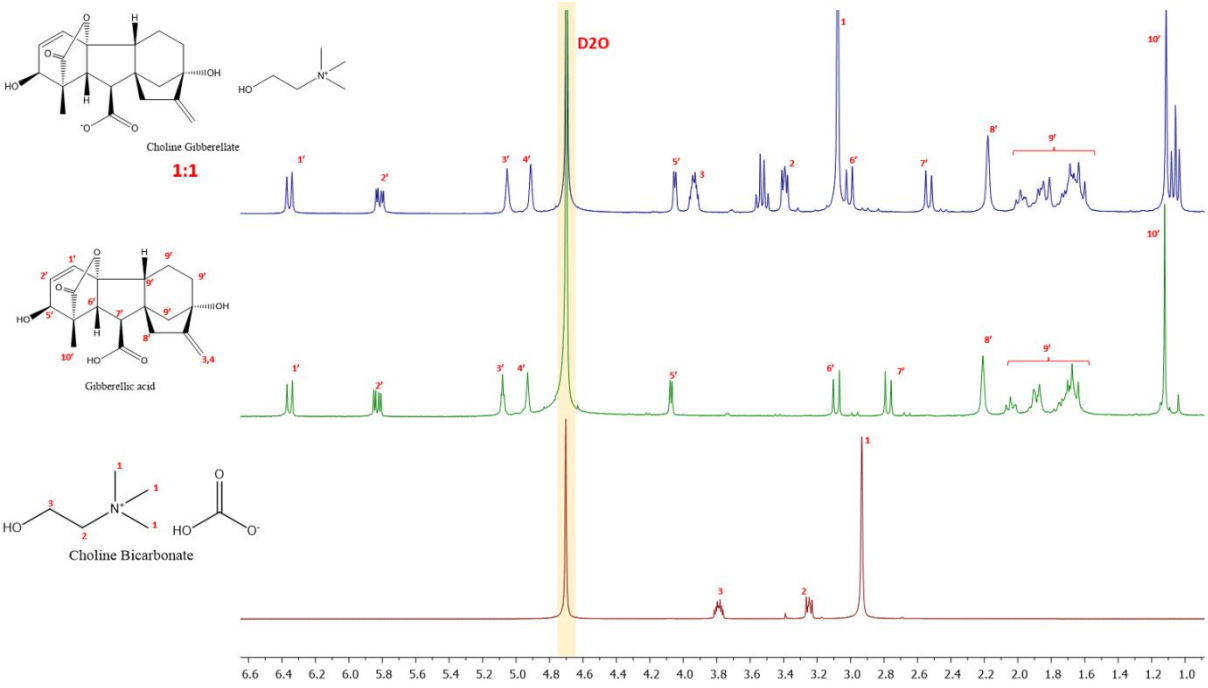
Choline Gibberellate
1:1
Gibberellic acid
Choline Bicarbonate
D2O
6.6 6.4 6.2 6.0 5.8 5.6 5.4 5.2 5.0 4.8 4.6 4.4 4.2 4.0 3.8 3.6 3.4 3.2 3.0 2.8 2.6 2.4 2.2 2.0 1.8 1.6 1.4 1.2 1.0

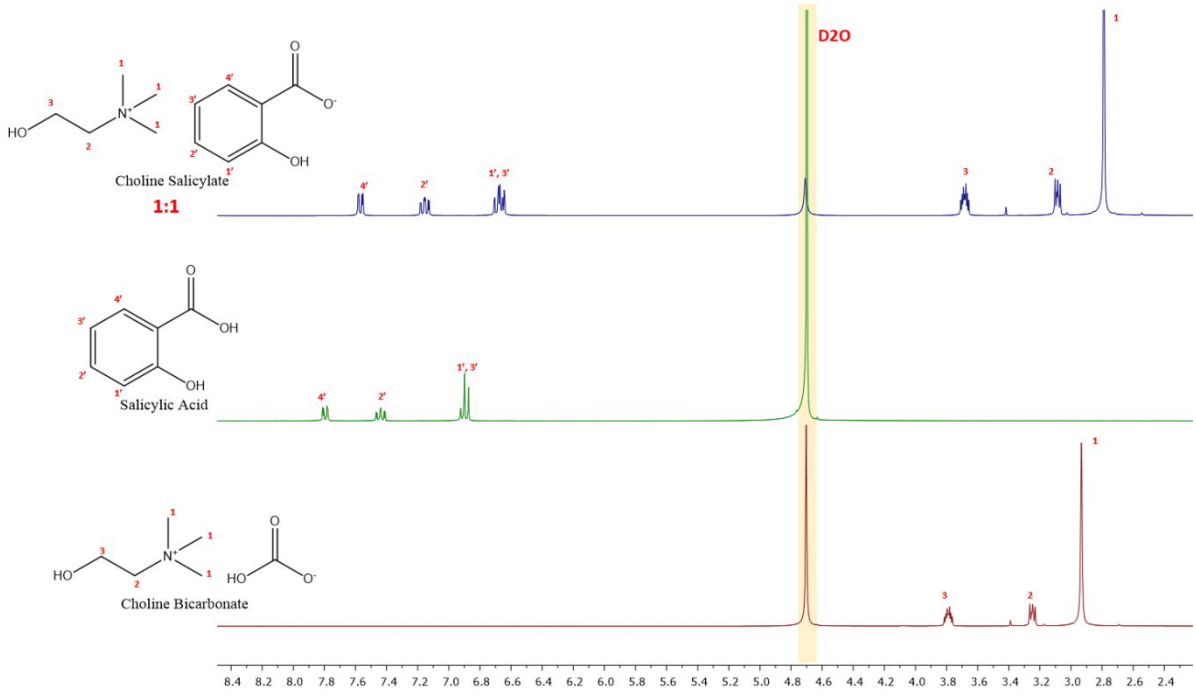


**Figure S1.** $^{1}H$ NMR spectra of the pure precursors and of the synthetized ionic liquids.

**Section III: Suspensions preparation**

**Table S1.** Initial ionic liquid and copper oxide concentrations of the suspensions prepared for the ion release profile experiments.

| Suspensions | IL / mM | CuO / ppm |
|---|---|---|
| $H_2O$ + CuO | - | 110 |
| $H_2O$ + [Cho][Asc] + CuO | 10.3 | 112 |
| $H_2O$ + [Cho][IAA] + CuO | 10.1 | 102 |
| $H_2O$ + [Cho][IBA] + CuO | 8.4 | 100 |
| $H_2O$ + [Cho][$GA_3$] + CuO | 4.3 | 112 |
| $H_2O$ + [Cho][Sal] + CuO | 9.4 | 107 |

**Table S2.** Initial ionic liquid and copper oxide concentrations of the suspensions prepared for the plant application experiments.

| Suspensions | IL / mM | CuO / ppm |
|---|---|---|
| $H_2O$ + [Cho][Asc] | 9.8 | - |
| $H_2O$ + [Cho][IBA] | 8.7 | - |
| $H_2O$ + [Cho][$GA_3$] | 5.0 | - |
| $H_2O$ + [Cho][Sal] | 10.7 | - |
| $H_2O$ + CuO | - | 112 |
| $H_2O$ + [Cho][Asc] + CuO | 9.8 | 179 |
| $H_2O$ + [Cho][IBA] + CuO | 8.5 | 175 |
| $H_2O$ + [Cho][$GA_3$] + CuO | 4.8 | 92 |
| $H_2O$ + [Cho][Sal] + CuO | 10.7 | 116 |

**Section IV: Ion release profiles and NPs characterization**

**Table S3.** Dissolution of copper ions in different mediums as a function of time.

| Suspensions / t / h | Copper ions concentration / ppb | | | | | |
|---|---|---|---|---|---|---|
| | **1** | **6** | **12** | **24** | **72** | **168** |
| $H_2O$ + CuO | 7 ± 2 | 16 ± 2 | 23 ± 1 | 36 ± 1 | - | 61 ± 1 |
| $H_2O$ + [Cho][Asc] + CuO | 115 ± 8 | 716 ± 18 | 1176 ± 19 | 1491 ± 40 | 4310 ± 142 | 36369 ± 1238 |
| $H_2O$ + [Cho][IAA] + CuO | 5 ± 1 | 9 ± 1 | 17 ± 2 | 24 ± 2 | 34 ± 1 | 55 ± 3 |
| $H_2O$ + [Cho][IBA] + CuO | 4 ± 1 | 6 ± 1 | 11 ± 1 | 19 ± 1 | 33 ± 1 | 58 ± 5 |
| $H_2O$ + [Cho][$GA_3$] + CuO | 4 ± 2 | 7 ± 1 | 13 ± 1 | 17 ± 2 | 28 ± 1 | 65 ± 4 |
| $H_2O$ + [Cho][Sal] + CuO | 138 ± 5 | 528 ± 20 | 1304 ± 44 | 2579 ± 124 | 6343 ± 360 | 12459 ± 427 |

**Table S4.** D-spacing values from the crystalline structure of copper oxide obtained from HR-TEM, and directly measured with the ImageJ software.

| | Length / nm | |
|---|---|---|
| | **CuO** | **CuO + [Cho][Sal]** |
| 1 | 0.229 | 0.335 |
| 2 | 0.236 | 0.285 |
| 3 | 0.229 | 0.310 |
| 4 | 0.296 | 0.273 |
| 5 | 0.244 | 0.310 |
| 6 | 0.278 | 0.285 |
| 7 | 0.280 | 0.273 |
| 8 | 0.325 | 0.223 |
| 9 | 0.313 | 0.273 |
| 10 | 0.252 | 0.323 |
| 11 | 0.261 | 0.298 |
| 12 | 0.227 | 0.248 |
| 13 | 0.252 | 0.260 |
| 14 | 0.261 | 0.248 |
| 15 | 0.323 | 0.273 |
| 16 | 0.313 | 0.273 |
| 17 | 0.304 | 0.248 |
| 18 | 0.304 | 0.260 |
| 19 | 0.304 | 0.211 |
| 20 | 0.288 | 0.248 |
| 21 | 0.252 | 0.273 |
| 22 | 0.323 | 0.261 |
| 23 | 0.261 | 0.248 |
| 24 | 0.270 | 0.298 |
| 25 | 0.261 | 0.260 |
| **Mean** | 0.276 | 0.272 |
| **SD** | 0.032 | 0.029 |
| **Min** | 0.227 | 0.211 |
| **Max** | 0.325 | 0.335 |

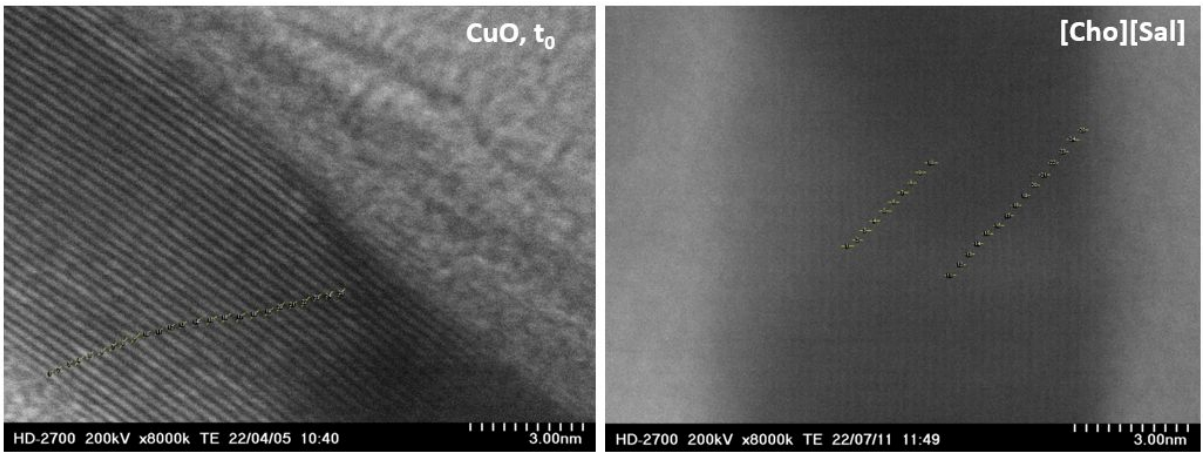


**Figure S2.** High-resolution TEM images showing lattice spacing of CuO nanoparticles before the ion release profile experiments (left panel), and of non-dissolved CuO after the dissolution kinetics in [Cho][Sal] (right panel).

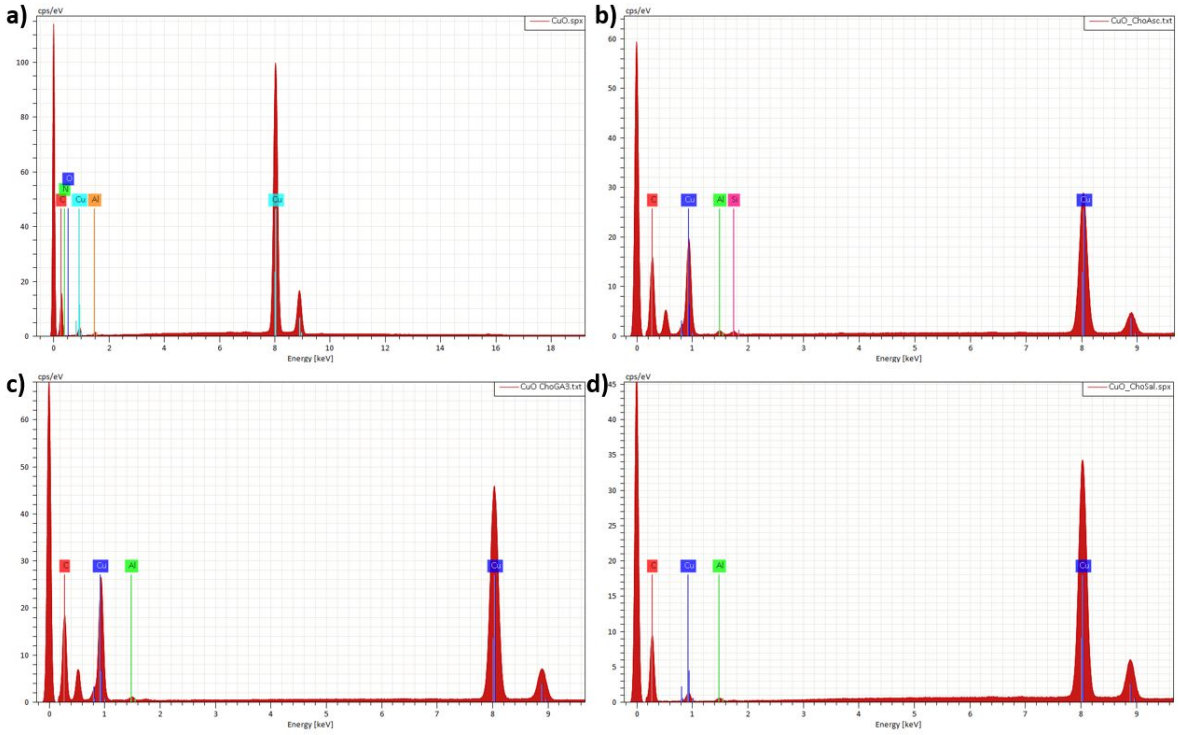


**Figure S3.** EDS spectra of: a) CuO before the ion release profile experiments; and non-dissolved CuO after dissolution kinetics in: b) [Cho][Asc]-based medium, c) [Cho][$GA_3$]-based medium, d) [Cho][Sal]-based medium.

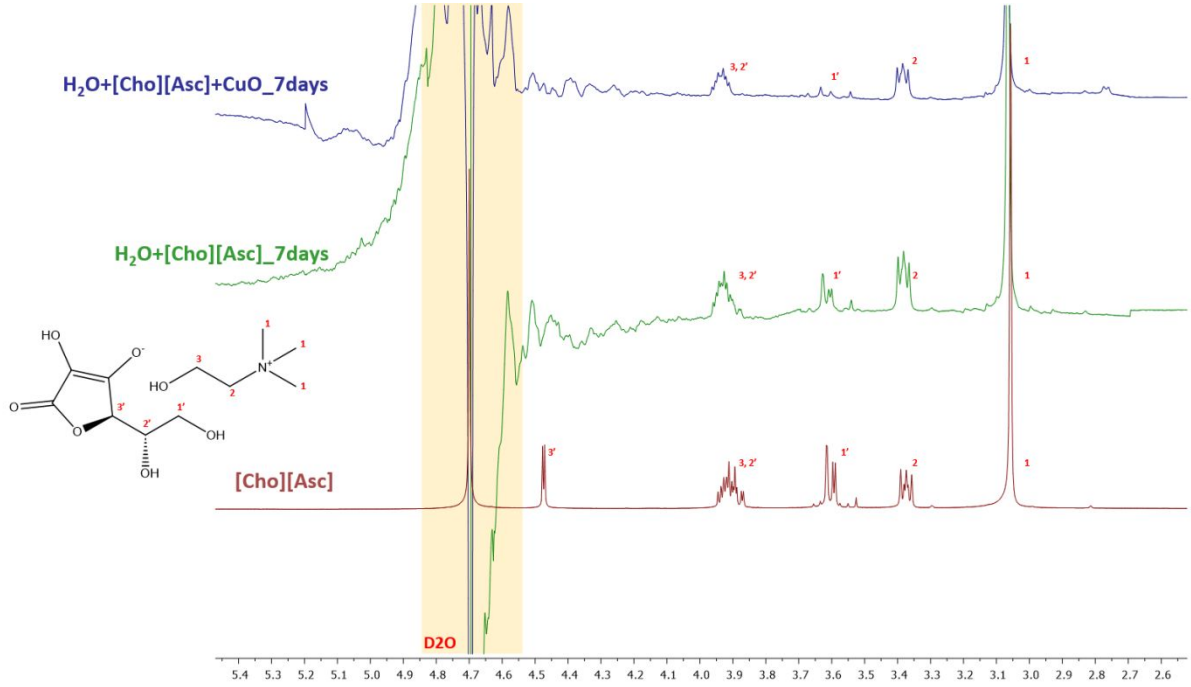


**Figure S4.** $^{1}$H NMR spectra of pure [Cho][Asc], and aqueous [Cho][Asc] and [Cho][Asc]+CuO, after 7 days kinetics. The $^{1}$H NMR spectra of the water phase was evaluated by suppressing the water peak.

## Section V: Plant application

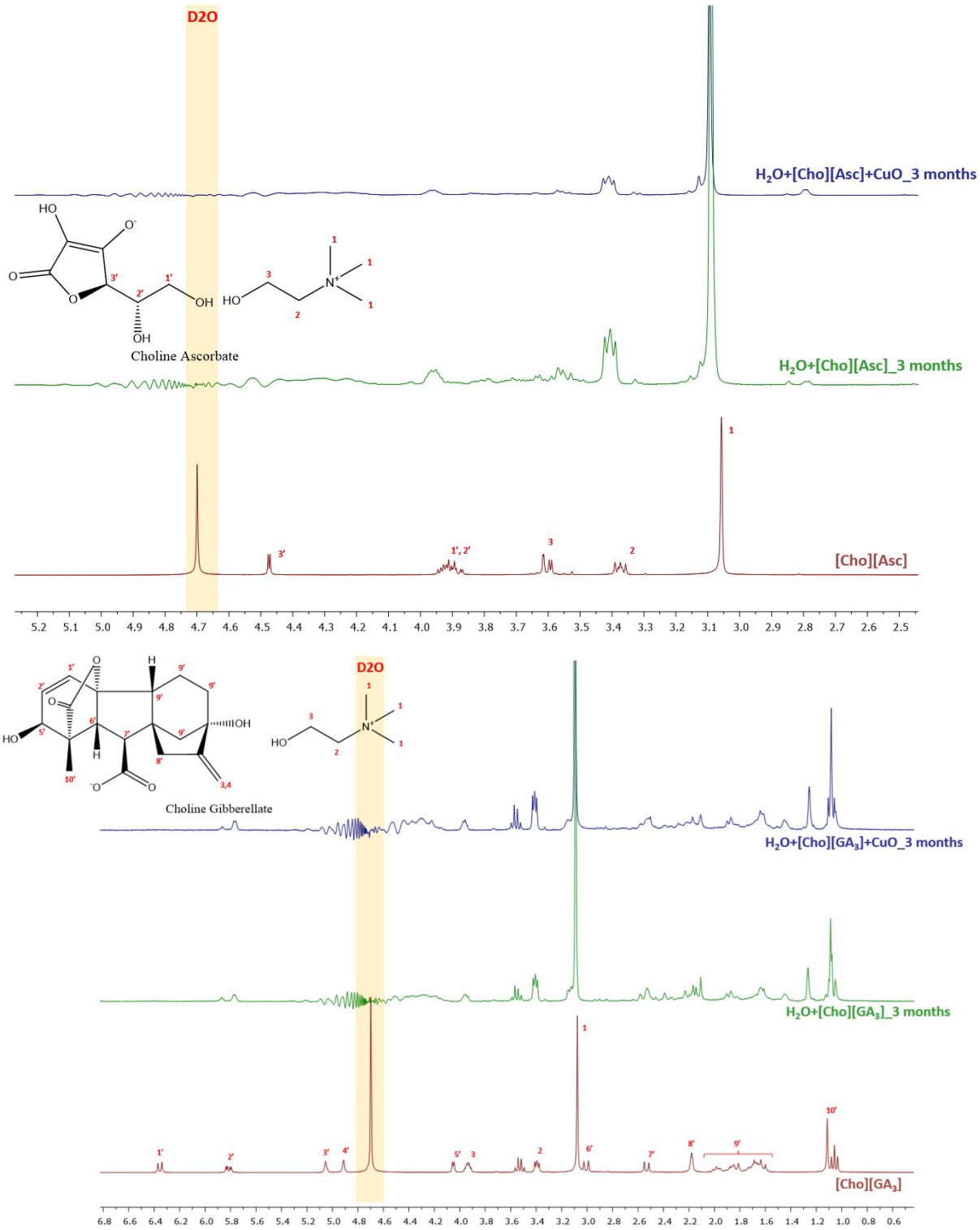

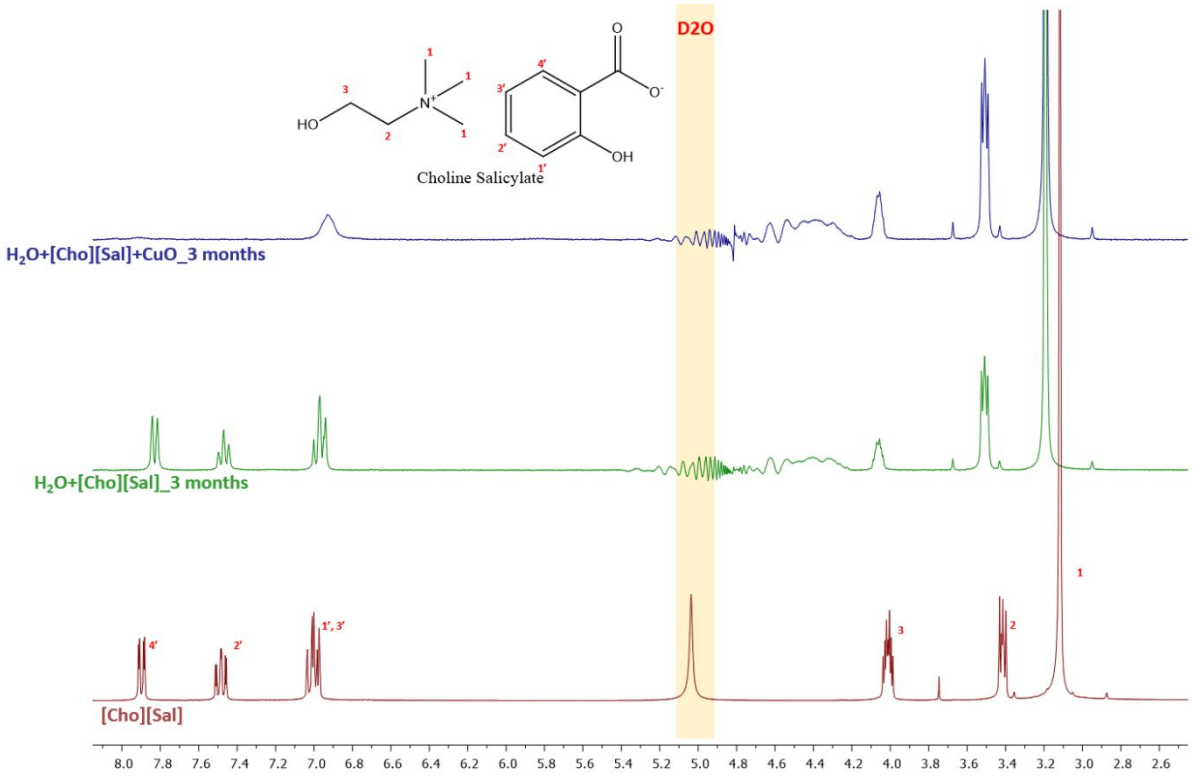


**Figure S5.** $^{1}$H NMR spectra of pure ILs and their mixtures with water and CuO, prepared following the procedure described in section 2.5.1 in the experimental section of the manuscript, after 3 months. The $^{1}$H NMR spectra of the water phase was evaluated by suppressing the water peak.

## References


(1) Mondal, D.; Sharma, M.; Mukesh, C.; Gupta, V.; Prasad, K. Improved Solubility of DNA in Recyclable and Reusable Bio-Based Deep Eutectic Solvents with Long-Term Structural and Chemical Stability. *Chem. Commun.* **2013**, *49* (83), 9606–9608. https://doi.org/10.1039/C3CC45849K.

(2) Sharma, M.; Mondal, D.; Sequeira, R. A.; Talsaniya, R. K.; Maru, D. A.; Moradiya, K.; Prasad, K. Syntheses and Characterization of Few Bio-Ionic Liquids Comprising of Cholinium Cation and Plant Derived Carboxylic Acids as Anions. *J. Indian Chem. Soc.* **2021**, *98* (11), 100205. https://doi.org/10.1016/J.JICS.2021.100205.

(3) Ma, C.; Borgatta, J.; Hudson, B. G.; Tamijani, A. A.; De La Torre-Roche, R.; Zuverza-Mena, N.; Shen, Y.; Elmer, W.; Xing, B.; Mason, S. E.; Hamers, R. J.; White, J. C. Advanced Material Modulation of Nutritional and Phytohormone Status Alleviates Damage from Soybean Sudden Death Syndrome. *Nat. Nanotechnol.* **2020**, *15* (12), 1033–1042. https://doi.org/10.1038/s41565-020-00776-1.

(4) Borgatta, J.; Ma, C.; Hudson-Smith, N.; Elmer, W.; Plaza Pérez, C. D.; De La Torre-Roche, R.; Zuverza-Mena, N.; Haynes, C. L.; White, J. C.; Hamers, R. J. Copper Based Nanomaterials Suppress Root Fungal Disease in Watermelon ( Citrullus Lanatus ): Role of Particle Morphology, Composition and Dissolution Behavior. *ACS Sustain. Chem. Eng.* **2018**, *6* (11), 14847–14856. https://doi.org/10.1021/acssuschemeng.8b03379.

(5) Martins, M. A. R.; Silva, L. P.; Ferreira, O.; Schröder, B.; Coutinho, J. A. P.; Pinho, S. P. Terpenes Solubility in Water and Their Environmental Distribution. *J. Mol. Liq.* **2017**, *241*, 996–1002. https://doi.org/10.1016/j.molliq.2017.06.099.

(6) Misra, S. K.; Dybowska, A.; Berhanu, D.; Croteau, M. N.; Luoma, S. N.; Boccaccini, A. R.; Valsami-Jones, E. Isotopically Modified Nanoparticles for Enhanced Detection in Bioaccumulation Studies. *Environ. Sci. Technol.* **2012**, *46* (2), 1216–1222. https://doi.org/10.1021/es2039757.

(7) Dialysis tubing cellulose membrane avg. flat width 10 mm (0.4 in.) | Sigma-Aldrich https://www.sigmaaldrich.com/PT/en/product/sigma/d9277 (accessed Feb 5, 2023).

(8) Peharec Štefanić, P.; Košpić, K.; Lyons, D. M.; Jurković, L.; Balen, B.; Tkalec, M. Phytotoxicity of Silver Nanoparticles on Tobacco Plants: Evaluation of Coating Effects on Photosynthetic

Performance and Chloroplast Ultrastructure. *Nanomaterials* **2021**, *11* (3), 744. https://doi.org/10.3390/nano11030744.

(9) Murashige, T.; Skoog, F. A Revised Medium for Rapid Growth and Bio Assays with Tobacco Tissue Cultures. *Physiol. Plant.* **1962**, *15* (3), 473–497. https://doi.org/10.1111/j.1399-3054.1962.tb08052.x.

(10) Mondal, D.; Ghosh, A.; Prasad, K.; Singh, S.; Bhatt, N.; Zodape, S. T.; Chaudhary, J. P.; Chaudhari, J.; Chatterjee, P. B.; Seth, A.; Ghosh, P. K. Elimination of Gibberellin from Kappaphycus Alvarezii Seaweed Sap Foliar Spray Enhances Corn Stover Production without Compromising the Grain Yield Advantage. *Plant Growth Regul.* **2015**, *75* (3), 657–666. https://doi.org/10.1007/s10725-014-9967-z.